Forecasting Development

Forecasting Research Technical Report No. 363

Turbulence in the Neighbourhood of Thunderstorm Clouds

By D.J. Hoad

September 2001

Met Office , Forecasting Development , Room R321, London Road , Bracknell , Berkshire ,RG12 2SZ,
United Kingdom

00/0486

Forecasting Research
Technical Report No. 363

Turbulence in the Neighbourhood of Thunderstorm Clouds

by

D.J. Hoad

September 2001

The Met Office
Forecasting Development
Room R309
London Road
Bracknell
RG12 2SZ
United Kingdom

Met Office , Forecasting Development , Room R309, London Road , Bracknell , Berkshire ,RG12 2SZ, United Kingdom

Turbulence in the Neighbourhood of Thunderstorm Clouds
by
D. J. Hoad, Aviation Applications

Abstract

Thunderstorm (cumulonimbus) clouds pose many hazards to aircraft, including clear air turbulence caused by gravity waves generated by the storm. In addition, other less organised regions of turbulence around cumulonimbus clouds may also exist. It is not known how far turbulence that affects aircraft extends around a cumulonimbus cloud. Consequently, there is very little guidance as to the safe distance, both horizontal and vertical, by which such clouds should be avoided.

This study performed a preliminary investigation into the extent of turbulence around and above a cumulonimbus cloud (rather than within the cloud or beneath it), which could affect aircraft. This investigation was performed by simulating some cumulonimbus clouds using the Met Office's "Large Eddy Model" (LEM) with a variety of conditions. The results give an idea of the pattern of turbulence around a cumulonimbus cloud. Unfortunately the simulations were very limited and used idealised initial conditions. Therefore many more simulations should be performed before any firm conclusions can be made.

Contents

1 Introduction 3
2 Basics of Thunderstorm Development 3
2.1 Temperature profile and CAPE 3
1.2 Wind shear 5
3 The Large Eddy Model 6
4 The Simulations 8
4.1 Control Run 8
4.1.2 Analysis using different turbulence parameters 8
4.1.1 Lifetime of cloud 11
4.2 Investigating the Effect of Grid Resolution 11
4.3 Simulation with less Convective Available Potential Energy (CAPE) 13
4.4 Simulations with wind shear 14
4.4.1 Mid-latitude squall line 14
4.4.2 Tropical squall line 16
5 Conclusion and Recommendations for Further Work 18
References 19
Acknowledgements 19

1 Introduction

Thunderstorm (cumulonimbus) clouds pose many hazards to aircraft. One of these hazards is the turbulence within the cloud itself due to updraughts and downdraughts. Pilots are aware of this hazard and generally avoid flying through cumulonimbus clouds. The dangers of flying beneath a downdraught (or a “microburst”) when in close proximity to the ground are also well known. The updraught and downdraught motions in cumulonimbus clouds also generate gravity waves, which propagate out from the anvil, top of the cloud and the side of the cloud. These gravity waves can cause clear air turbulence some distance away from the storm. Besides these features, other less organised regions of turbulence may also exist. It is not known how far turbulence that affects aircraft extends around a cumulonimbus cloud. Consequently, there is very little guidance as to the safe distance, both horizontal and vertical, by which such clouds should be avoided.

The aim of this study was to perform a preliminary investigation into the extent of turbulence around and above a cumulonimbus cloud (rather than within the cloud or beneath it), which could affect aircraft. This investigation was performed by simulating some cumulonimbus clouds using the Met Office’s “Large Eddy Model” (LEM) with a variety of conditions.

This paper is split into 5 sections. The next section describes the basics of thunderstorm development. The following section gives an overview of the Large Eddy Model, which was used to simulate a cumulonimbus cloud. Then follows a description of the simulations performed and an analysis of the results. The paper then finishes with a brief conclusion.

2 Basics of Thunderstorm Development

In order to choose initial conditions for simulating thunderstorm clouds, a basic understanding of thunderstorm development and parcel theory is needed. Thunderstorm severity is determined by two factors: the temperature profile and the wind shear.

2.1 Temperature profile and CAPE

Thunderstorms may occur if the atmosphere is convectively unstable. In these conditions, if a parcel of air rises due to surface heating, it will continue to rise whilst it is warmer than the surrounding air.

The temperature profile can be plotted on a thermodynamic diagram such as the tephigram (Figure 1). Several types of lines are contained on the tephigram, and these are explained in Figure 2. A tephigram can also be used to plot the path of a rising parcel of air in convectively unstable conditions, as demonstrated in Figure 3. While the parcel is unsaturated, it will follow a dry adiabat line (θ = constant), until it becomes saturated. The point of saturation (and hence the base of the cloud) can be found by plotting the parcel’s ascent from the surface along a dry adiabat line. Because the water vapour in the rising parcel of air is conserved, another line can be drawn parallel to the saturation humidity mixing ratio (r = constant) lines from the surface dew point. The point where these two lines cross is the point of condensation. After the parcel has condensed, it will follow the saturated adiabat (θ_w = constant) line. The parcel of air will continue to rise if its path is to the right of the temperature profile, because it is warmer than the surrounding air. It will rise until its path crosses the temperature profile again, where

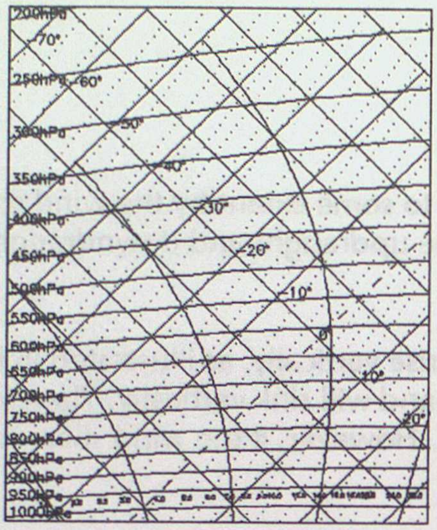

Figure 1. An example of a tephigram.

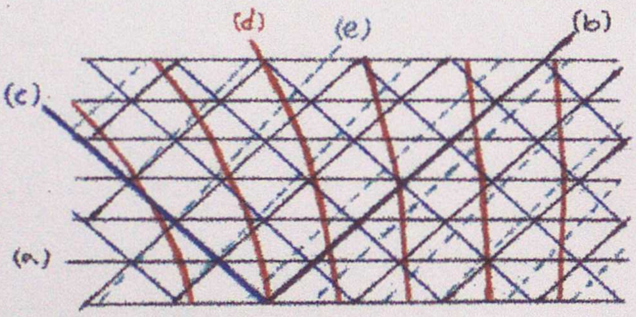

Figure 2. An illustration of the types of lines on a tephigram:
(a) Lines of equal pressure (isobars),
(b) lines of equal temperature (isotherms),
(c) dry adiabat (θ = constant) lines,
(d) saturated adiabat (θ_w = constant) lines,
and (e) saturation humidity mixing ratio (r = constant) lines.
(Adapted from a similar diagram provided Howard Lyne.)

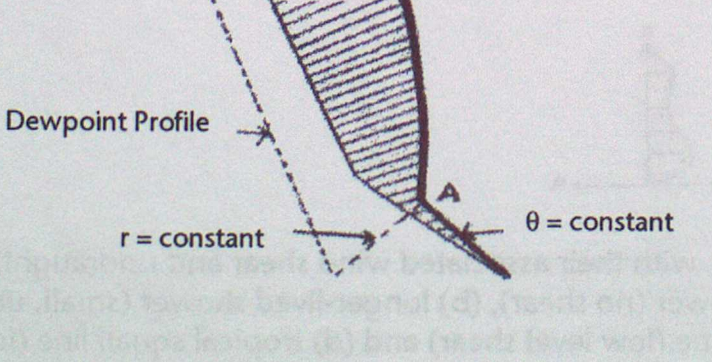

Figure 3. Plotting the ascent of a parcel of air in convectively unstable conditions. A is the point of condensation (and cloud base), B the point where the parcel of air becomes negatively bouyant (and where most of the cloud tops would be) and the shaded region is Convective Available Potential Energy (CAPE). (Adapted from a similar diagram provided by Howard Lyne.)

it will become colder than the surrounding air (and so the buoyancy force acting on it will become negative).

1.2 Wind shear

Whether the storm is actually severe or not is determined to some extent by the wind shear. This is because the wind shear affects the interaction of the updraught and downdraught of the storm, which determines the longevity of the storm.

For example, if there is no wind shear, the air parcels will rise vertically, as illustrated in Figure 4 a). The downdraught will develop over the inflow region and will sink vertically. Therefore it will eventually cut off the flow of warm air into the cloud. However, if the wind shear is such

(a) Short-lived shower (no shear)

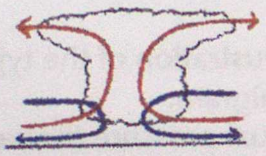

(b) Longer-lived shower

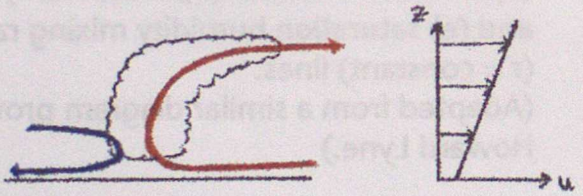

(c) Mid-latitude squall line

(d) Tropical squall line

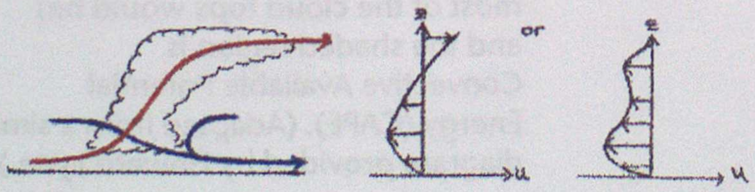

Figure 4. Different types of thunderstorms, with their associated wind shear and updraught/ downdraft interactions. (a) Short-lived shower (no shear), (b) longer-lived shower (small, uni-directional shear), (c) mid-latitude squall line (low level shear) and (d) tropical squall line (low-level jet). The blue arrows represent the downdraughts and the red arrows the updraughts.

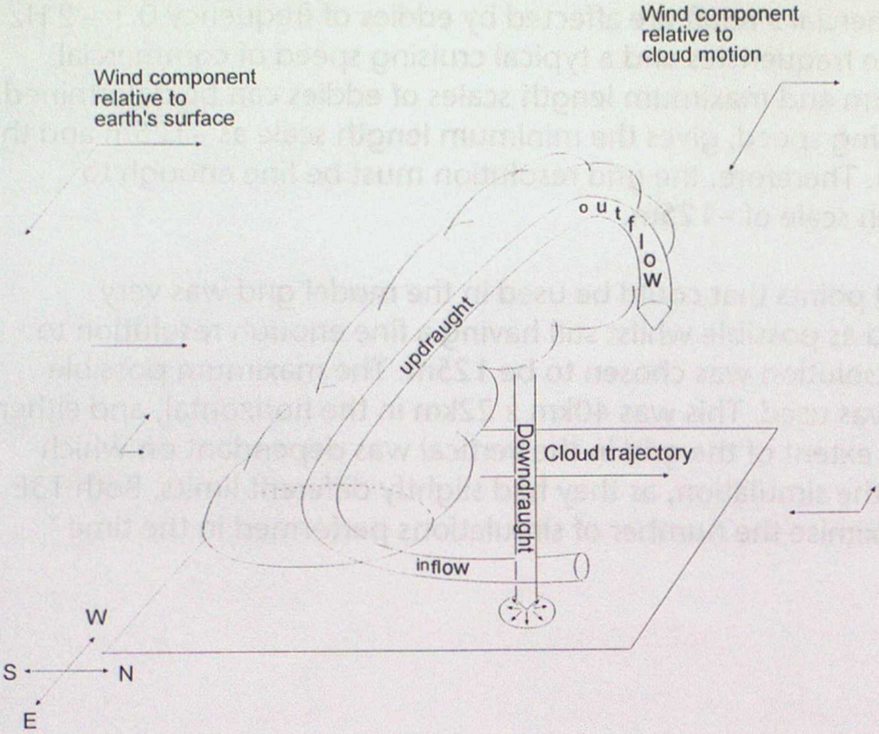

Figure 5. Diagram of a multicell storm showing the interaction of the updraught and the downdraught. (Courtesy of Howard Lyne, the Met Office College.)

that the downdraught does not develop over the core of the updraught, and falls to the other side of the cloud to the inflow of warm air to the cloud, as in Figure 4(c) for example, the cloud will be longer lived.

Figures 4 a), b), c), and d) show several types of one-dimensional wind shear with their corresponding thunderstorm type. If the wind changes direction with height, the downdraught falls to one side of the inflow of warm air and a muli-cell storm may develop. This type of storm is illustrated in Figure 5.

In this project, two types of wind shear were studied: those that are associated with the formation of a mid-latitude squall line and a tropical squall line.

3 The Large Eddy Model

The Met Office's Large Eddy Model (LEM) is a model which is used to simulate and investigate cumulonimbus clouds. A detailed description of the model can be found in S.H. Derbyshire et al. (1994). The core part of the model contains the physics required to solve a simple dry turbulence problem. The model has modules of extra code which deal with microphysical interactions and radiation. The model runs on the Met Office's supercomputer, the T3E. In the experiments performed in this study, the following input was needed:

- grid details (horizontal and vertical resolution);
- profile of temperature humidity and wind;
- the size of the cold pool or warm bubble to initialise the storm;
- the temperature anomaly of the cold pool or warm bubble.

The simulations used in these investigations were run using periodic boundary conditions.

The grid resolution used in the simulations was determined by considering the length scales of eddies which affect aircraft. Commercial aircraft are affected by eddies of frequency 0.1 – 2 Hz (Cornman et al. 1993). Using these frequencies and a typical cruising speed of commercial aircraft, an estimate of the minimum and maximum length scales of eddies can be determined. Using 250 ms^{-1} as the typical cruising speed, gives the minimum length scale as ~125m and the maximum length scale as ~2.5 km. Therefore, the grid resolution must be fine enough to identify eddies which have a length scale of ~125m.

Unfortunately, the number of grid points that could be used in the model grid was very restricted. So, to get as large a grid as possible whilst still having a fine enough resolution to identify the smallest eddies, the resolution was chosen to be 125m. The maximum possible grid domain with this resolution was used. This was 40km x 22km in the horizontal, and either 15km or 20km in the vertical. The extent of the grid in the vertical was dependant on which T3E supercomputer was used for the simulation, as they had slightly different limits. Both T3E supercomputers were used to maximise the number of simulations performed in the time allocated for the study.

The initialising conditions

A standard set of initialising conditions were used in the simulations (except where stated otherwise), and these are described in Tables 1 and 2. The standard temperature profile is also illustrated in Figure 6. The standard temperature profile was obtained from the Met Office's numerical weather prediction model, from a gridpoint in the tropics, where the fraction of convective cloud was greater than 0.4. The humidity profile was artificially moist in the simulations, because initial tests showed that the cloud dissipated too quickly otherwise.

Parameter	Value
Temperature Anomaly of cold pool	-2 °C
Width of cold pool	2000 m
Height of centre of cold pool	500m

Table 1. Dimensions of the initialising cold pool.

Pressure (mb)	Temperature (°C)	Humidity (%)
1000	29.7	89.2
950	24.3	96.4
925	22.7	98.1
900	21.2	99.5
850	18.2	99.7
700	9.9	99.7
600	3.9	97.6
500	-3.5	95.3
400	-14.5	80.0
300	-28.2	70.0
250	-33.0	5.0
150	-33.0	5.0
100	-31.0	5.0
70	-28.0	5.0
50	-25.0	5.0
30	-21.0	5.0
10	-18.0	5.0

Table 2. The standard temperature profile used in most of the simulations.

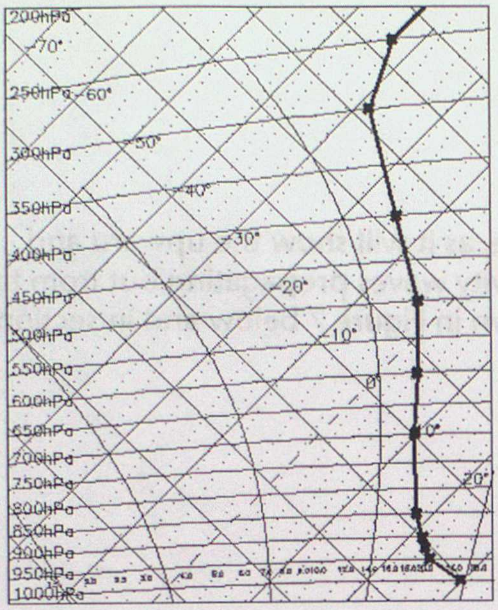

Figure 6. The standard temperature profile used in most of the simulations (plotted on a tephigram).

The other temperature profiles used in the simulations were also taken directly from or based on ones obtained from the Met Office's Numerical Weather Prediction model. The other humidity profiles were also based on ones obtained from the Numerical Prediction Model, but were made artificially moist, because the clouds in the early simulations dissipated too quickly.

The wind profiles used in the simulations were idealised. However, the maximum wind speed was restricted to 5 ms^{-1}, in order to try to keep the storm cloud on the grid. In the simulations with background wind, the initialising cold pool was positioned on the left or the right hand side of the grid, so the cloud would be roughly in the centre of the grid when the cloud is at the mature stage of it's life.

4 The Simulations

First, a control simulation was run using the standard initialising conditions and temperature/humidity profile described in the last section. Next, the effect of using different model grid resolutions was investigated. Then a comparison of two storms produced with different temperature/humidity profiles was performed. Lastly, two storms with different wind shears were studied.

4.1 Control Run

For this simulation, the model was run with no background wind (and hence no wind shear), using the standard initialising and background conditions described in Tables 1 and 2, and Figure 6.

4.1.2 Analysis using different turbulence parameters

Before analysing the results for the control run, the use of different turbulence parameters was investigated. The result for the control run 43 minutes after initiation was used for this investigation. The parameters investigated were:

i) vertical wind velocity, w
ii) average Turbulent Kinetic Energy (TKE)
iii) Bulk Richardson number

<u>i) Vertical wind velocity, w</u>

Vertical wind velocity is useful for analysing turbulence, as it will show the upward and downward motion associated with eddies and the gravity waves propagating out from the storm. Cross sections of vertical wind velocity are shown in Figure 7 below and in section 4.1.2.

<u>ii) Turbulent Kinetic Energy (TKE)</u>

Turbulent Kinetic Energy, TKE, is calculated using:

$$TKE = \frac{1}{2}(u'^2 + v'^2 + w'^2)$$

where
u'= perturbation of the x component of the wind (u)
v'= perturbation of the y component of the wind (v)
w'= perturbation of the z component of the wind (w)

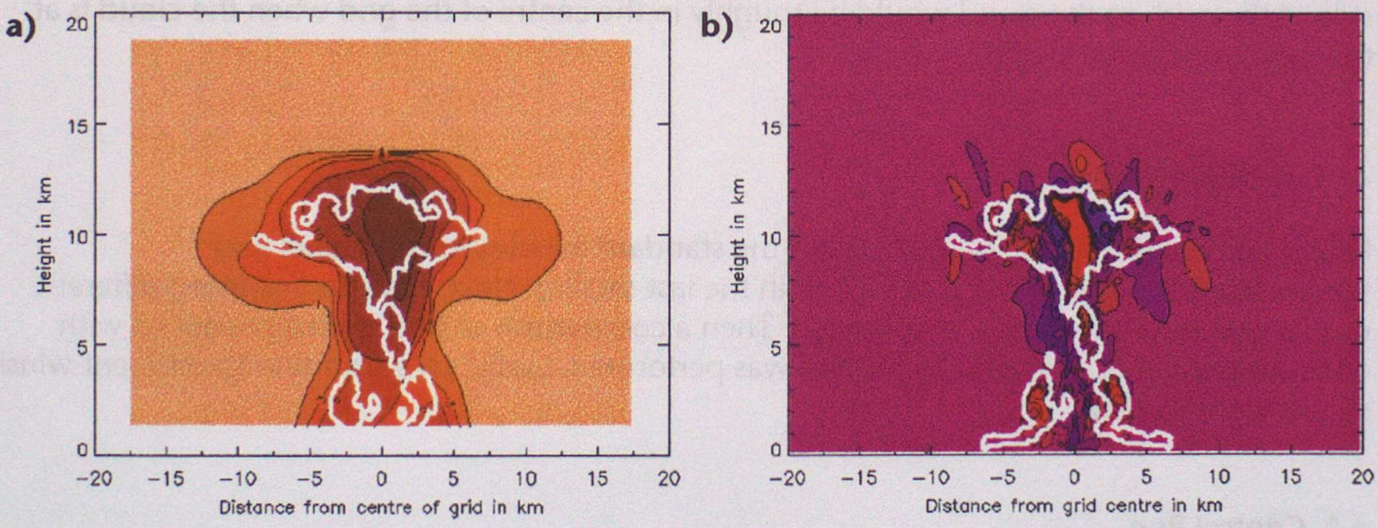

Figure 7: (a) Cross section (through a slice 1250m from the centre of the grid) of average turbulent kinetic energy, 43 minutes after initiation. Contours are drawn at intervals of 1, 3, 5,10, 20, 30 m^2s^{-2}. (b) The corresponding cross section of w, with contours are drawn at ± 1, 3, 5, 7 ms^{-1}, with red colours indicating positive values of w (i.e. updraughts) and the blue colours indicating negative values of w (i.e. downdraughts). The outline of the cloud is indicated by the thick white line (which is plotted where the sum of cloud liquid water content and cloud ice content is equal to 0.00001 gkg^{-1}). Note that the domain of the TKE plot is smaller than the domain of the vertical wind plot; this is because the TKE has been averaged over 2.5 km x 2.5 km x 2.5 km cubes.

An average of TKE over a 2.5 km x 2.5 km x 2.5 km box was used in the analysis of the results. This was calculated by:

1) calculating the mean value of the wind components in 2.5 km x 2.5 km x 2.5 km cubes of the grid
2) then calculating the perturbation of u, v, and w at each gridpoint
3) then calculating the average TKE over in each 2.5 km x 2.5 km x 2.5km cube used in step 1.

Figure 7a) shows the cross-section of average turbulent kinetic energy, TKE (averaged over a cubic area 2.5 km x 2.5 km x 2.5 km), for the control run 43 minutes after initiation. This cross section was along the closest slice to the grid centre available, which was 1.25 km from the grid centre. The corresponding cross section of vertical wind speed is shown in Figure 7b) for comparison. The greatest magnitude of TKE occurred in the cloud and was about 50 m^2s^{-2}. The pattern of TKE around the cloud corresponded well with the extent of the gravity waves.

iii) The Bulk Richardson Number

The Bulk Richardson Number (Ri) is defined by:

$$Ri = \frac{g \Delta\theta \Delta z}{\theta[\Delta u^2 + \Delta v^2]}$$

where:
g= acceleration due to gravity
θ = potential temperature (can be calculated from pressure and temperature)
Δθ = change in potential temperature
Δu = change in x component of wind speed, u
Δv = change in y component of wind speed, v
z=height
Δz = change in height
If Ri is less than or equal to 0.25, the atmosphere is turbulent.

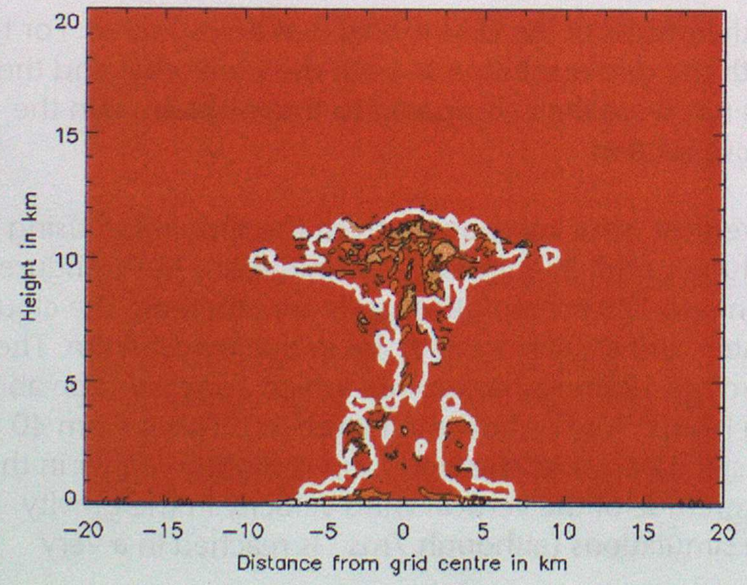

Figure 8: Cross section (through the centre of the grid) of bulk Richardson Number, 43 mins after initiation. Contours are drawn at 0, 0.25 and 1, with the yellow areas representing regions where Ri ≤ 0 and the dark orage area where Ri ≥ 1. The outline of the cloud is indicated by the thick white line, as in Figure 7.

The cross section of the bulk Richardson number 43 minutes after initiation is plotted in Figure 8. The areas where Ri ≤ 0.25 occur almost completely within the cloud, so this parameter is probably not very useful in this study.

It was decided to analyse and present the rest of the results in terms of the vertical wind velocity. This was because of several reasons. Firstly, the bulk Richardson number plot in this case was not helpful in identifying regions of turbulence outside the cloud. The plot of TKE was useful for identifying regions of turbulence around the cloud, but the plot of the vertical wind velocity was better because it shows the individual gravity waves, and the distance between the maxmium upward and downward velocity in the gravity waves can be determined. This can then be compared with the length scale estimates for turbulence which affect aircraft, to see if the gravity waves would cause turbulence which would affect aircraft.

4.1.1 Lifetime of cloud

Figure 9 shows the vertical wind velocity, w, at 4 times of the cloud's lifetime: when the cloud is developing, mature and dissipating. The gravity waves appear to be strongest at the mature stages of the cloud's life (young mature and old mature/dissipating). In this simulation, the strongest value of w in the gravity waves is ±7 ms^{-1}, which occurs above the cloud top. The wavelength of the gravity waves varies, from about 2.5 km to about 10km, with the larger wavelength gravity waves being produced from the side of the cloud and top of the cloud, and the smaller wavelength gravity waves being produced from the top of the anvil. These gravity waves would produce turbulence with length scales of about 1.25-5 km (this is the distance between the upward and downward wind maxims). Since the length scale of the turbulence that affects aircraft is 0.125–2.5 km, the shortest wavelength gravity waves will cause turbulence on the scale that it will affect aircraft. However, the magnitude of vertical velocity in these gravity waves is not very large (about 2-3 ms^{-1}) compared with the length scale, so that the turbulence in this case would be minor.

In this simulation, there is little or no turbulence surrounding the cloud system (apart from above the cloud).

4.2 Investigating the Effect of Grid Resolution

Next, the effect of the grid resolution on the results of the LEM model was investigated. For this investigation, the LEM model was run with the grid resolution in both the horizontal and the vertical set to 200m. The results from this run were then compared to those obtained in the control simulation described in the previous section.

Figure 10 compares the cross section of vertical wind component from the simulation using the 200m resolution grid and the 125m resolution grid, 33 minutes after initiation. As this figure shows, the results for the 200m resolution and 125 m resolution grids are different. The cloud in the coarser resolution run develops faster, and there is some noise in the lowest 4 km. The cross-section of vertical wind velocity from the 125m resolution run which appears to be about the same stage of development as that in Figure 10a) is shown in Figure 9c). This is from 40 minutes after initiation. The cloud shape still differs, and the cloud top is slightly higher in the fine resolution results. The maximum magnitude of the vertical wind velocity in the gravity waves is generally about ± 3 ms^{-1} in both simulations (although 7ms^{-1} is reached in a very

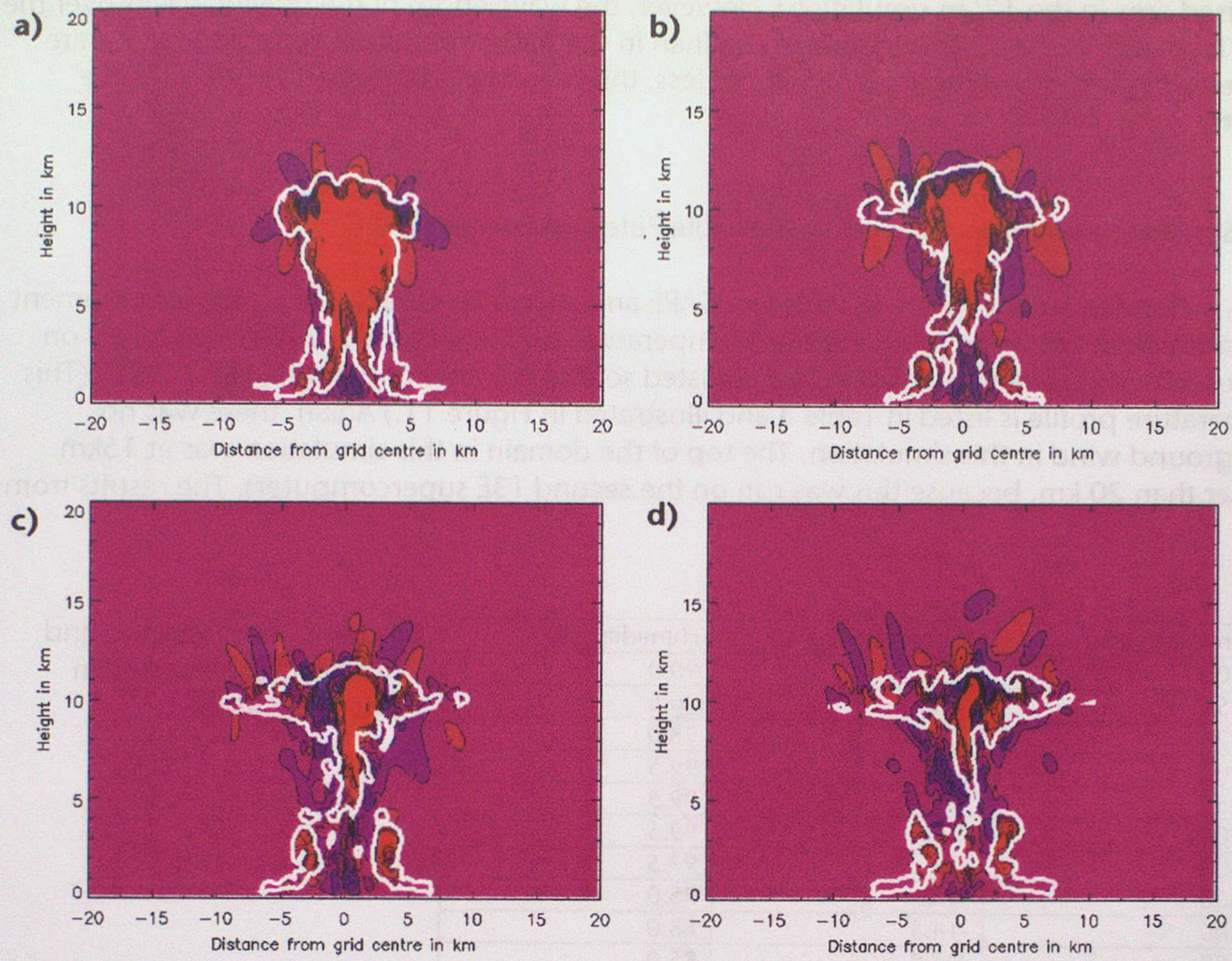

Figure 9: Cross section (through the centre of the grid) of vertical wind component (w) at 4 stages of the cloud's lifetime: (a) developing cloud (35 minutes after initiation), (b) young mature cloud (40 minutes after initiation), (c) old mature cloud (starting to dissipate) 43 minutes after initiation, (d) dissipating cloud (46 minutes after initiation). The contour intervals, colouring and outline of the cloud are as in Figure 7.

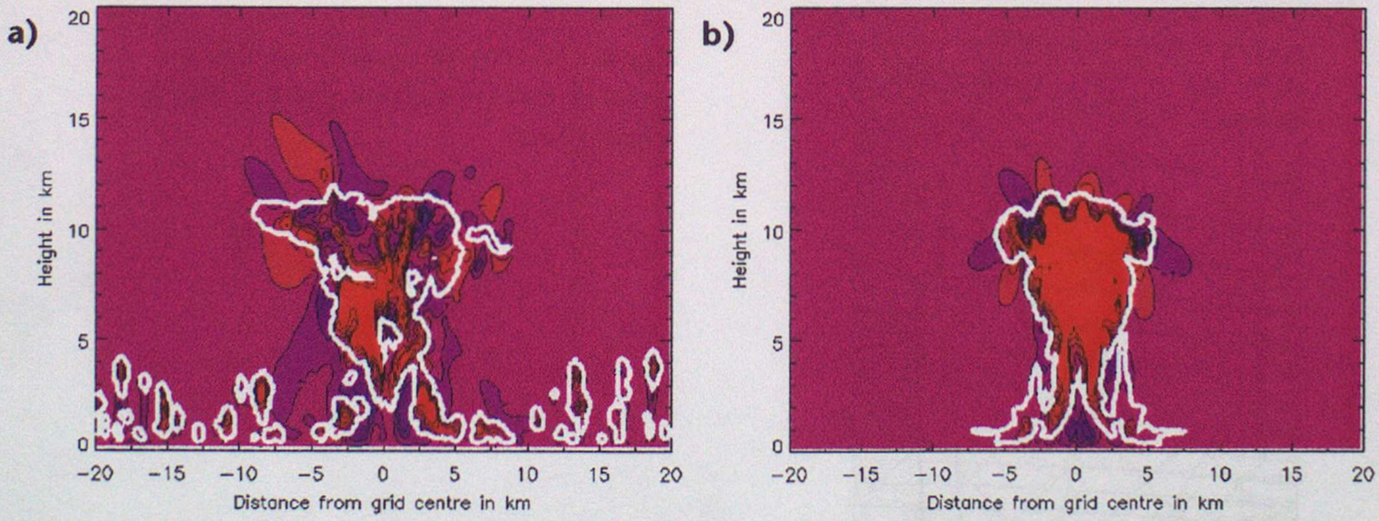

Figure 10: Comparison of results for different grid resolutions, 33 minutes after initiation. (a) Vertical wind component (w) for the coarse grid simulation. (b) Vertical wind component (w) for the fine grid simulation. The contour intervals, colouring and outline of the cloud are as in Figure 7.

localised area in the 125m simulation). However, the wavelength of the gravity waves over the anvil is smaller in the 125m resolution run than in the 200m resolution run; because we are interested in half wavelengths of 2.5 km or less, this is an important consideration for the results.

4.3 Simulation with less Convective Available Potential Energy (CAPE)

Next, a cloud in an environment with less CAPE and so less favourable for storm development was simulated. For this run, an idealised temperature profile was used, which was based on that used in the control simulation but adjusted so that the environment had less CAPE. (This temperature profile is listed in Table 3 and illustrated in Figure 11.) Again, there was no background wind in this simulation. The top of the domain in this simulation was at 15km (rather than 20 km, because this was run on the second T3E supercomputer). The results from

Pressure (mb)	Temperature (°C)	Humidity (%)
1000	27.0	90.0
950	24.5	96.5
925	22.0	98.0
900	20.5	99.5
850	18.5	99.5
700	10.5	99.5
600	4.5	97.5
500	-3.0	95.0
400	-14.5	88.0
300	-27.0	85.0
250	-37.0	80.0
150	-50.0	70.0
100	-45.0	5.0
70	-40.0	5.0
50	-34.0	5.0
30	-28.0	5.0
10	-24.0	5.0

Table 3. Temperature and humidity profile used in this simulation.

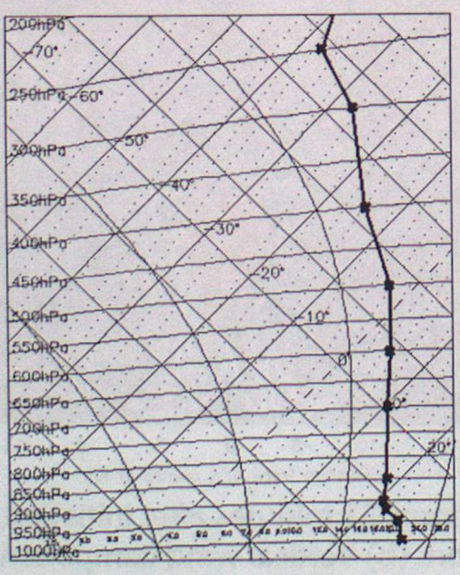

Figure 11. The temperature profile used in this simulation (plotted on a tephigram).

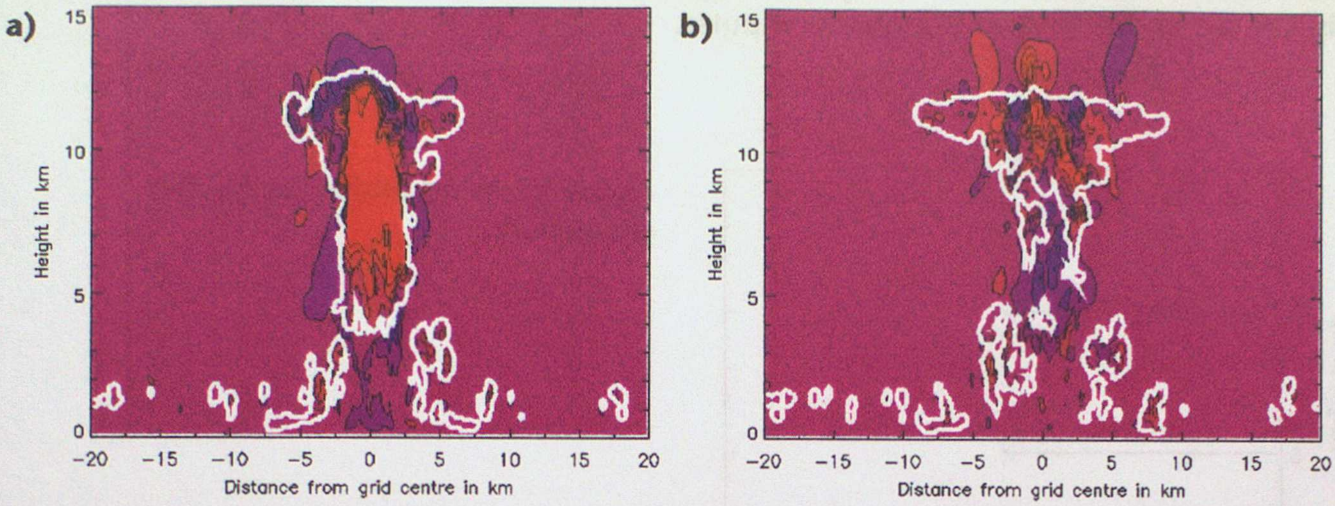

Figure12. Cross-section of vertical wind velocity (a) 43 minutes, (b) 50 minutes after initiation. The contour intervals, colouring and outline of the cloud are as in Figure 7.

this run were then compared to those obtained in the control simulation described in section 4.1.

Figure 12 shows the vertical wind component 43 minutes and 50 minutes after initiation, when the cloud is in the mature and dissipating stages of its life. The maximum magnitude of the vertical velocity in the gravity waves was about 7 ms^{-1}, occurring above the cloud top 50 minutes after initiation. However, in general, the magnitude of gravity wave vertical velocity is not very large (about 1-3 ms^{-1}). As before the wavelength of the gravity waves varies, from about 2.5 km to about 10 km, with the larger wavelength waves being produced from the side and top of the cloud, and the smaller wavelength waves being produced from the top of the anvil. The pattern of gravity waves produced from the side of the cloud is asymmetrical. This was unexpected because there was no wind shear in this simulation. This asymmetry is possibly due to the noise in the input moisture field (which contained noise in order to produce more turbulence), since the magnitude of vertical velocity in these gravity waves is of the order of 1 ms^{-1}.

In comparison to the control run (see Figure 9), the gravity waves produced over the anvil in this simulation are, in general, less well developed. However, the maximum vertical velocity in the gravity wave generated over the cloud top is comparable to that in the control run.

4.4 Simulations with wind shear

Lastly, the effect of wind shear was investigated. Two types of wind profiles were investigated: those that are associated with the development of midlatitude and tropical squall lines.

4.4.1 Mid-latitude squall line

For this simulation, the same temperature profile was used as in the control run (see Table 2 and Figure 6). An idealised uni-directional wind profile was used (illustrated in Figure 13), where the wind increased steadily from 0 ms^{-1} at the surface to 5 ms^{-1} at 1 km; above that the wind was constant at 5 ms^{-1}. The top of the domain in this simulation was at 15km, because this was run on the second T3E supercomputer.

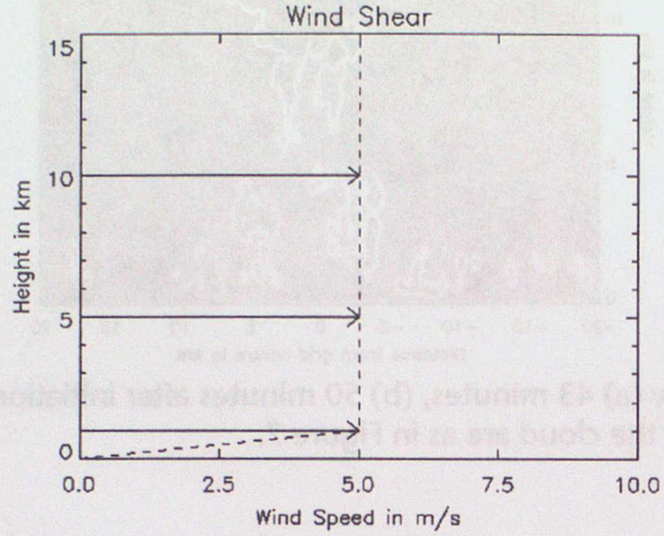

Figure 13. Wind profile used in this simulation.

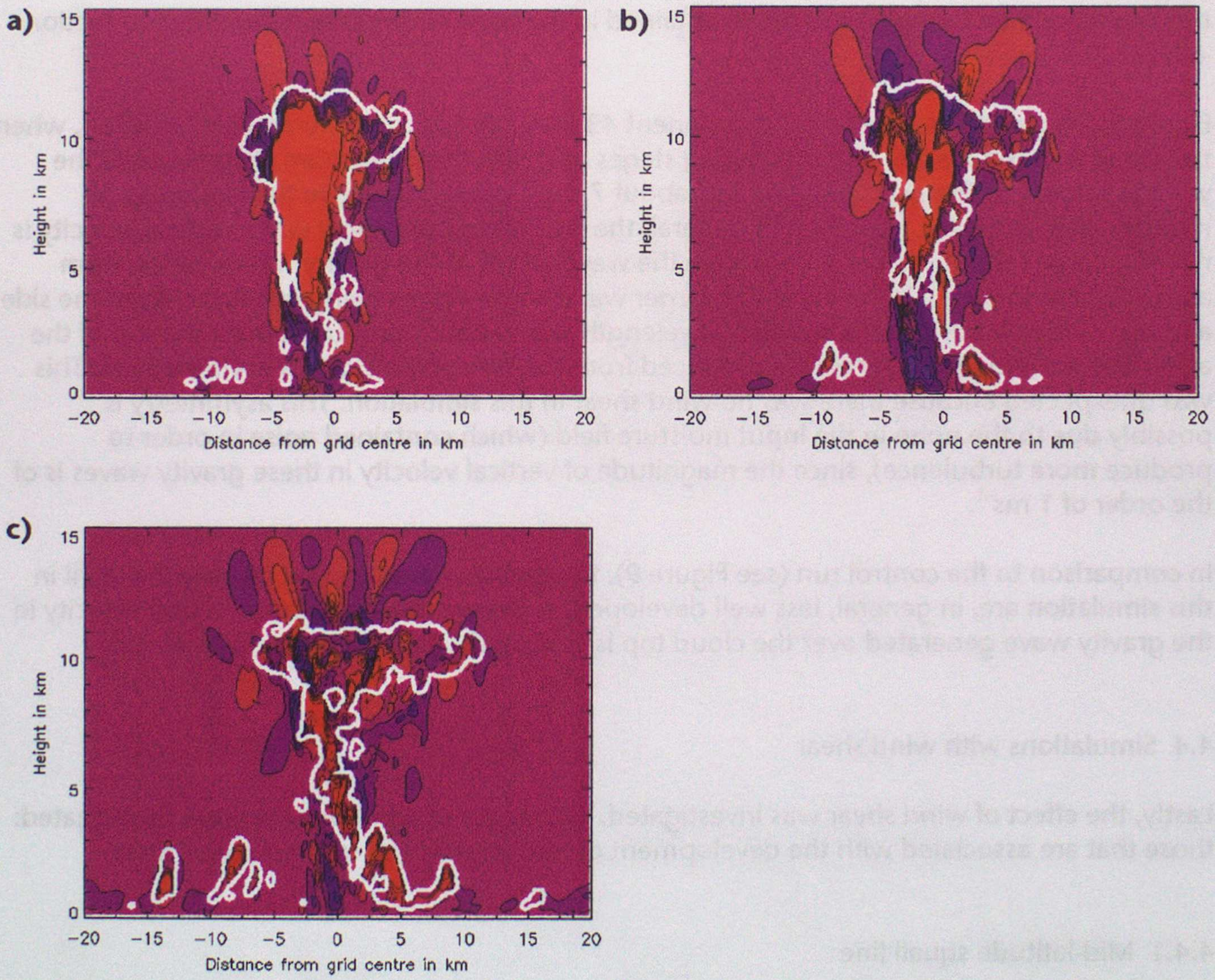

Figure 14. The vertical wind velocity (w) in ms^{-1} (a) 30 minutes, (b) 33 minutes and (c) 38 minutes after initiation. The contour intervals, colouring and outline of the cloud are as in Figure 7.

Figure 14 shows the vertical wind at 3 stages of the clouds lifetime: a) at 30 minutes, b) at 34 minutes and c) at 40 minutes after initiation. The plots are taken along the same slice through the centre of the grid as before, which was parallel to the direction of the wind shear in this simulation.

In this simulation, the maximum magnitude of the vertical velocity in the gravity waves was about ±7 ms^{-1}, occurring above the cloud during the mature and dissipating stages of the cloud's life. This is about the same as the maximum that occurred in the control simulation. Again, the wavelength of the gravity waves was variable, from about 2.5 km to about 5 km. The smallest wavelength gravity waves are on a small enough scale to cause turbulence to aircraft. These gravity waves were being produced from the top and underneath the anvil.

The gravity waves on the downwind side of the cloud propagate further than on the upwind side of the cloud.

This cloud was expected to last for longer because of the wind shear. However, it dissipated as fast as those in earlier simulations. This may be because the model atmosphere was extra moist, or because the magnitude of the wind shear was not very large.

4.4.2 Tropical squall line

For this simulation, a temperature profile very similar to that used for the control run was used, but differed in that the tropopause was much higher (this temperature profile is listed in Table 4 and illustrated in Figure 15). An idealised wind profile was used, where there were two maximums in wind speed, representing the African Easterly Jet and the Tropical Easterly Jet (although, unfortunately, the maximum wind speed was limited to 5ms^{-1} to keep the cloud on the grid). This profile is shown in Figure 16.

Pressure (mb)	Temperature (°C)	Humidity (%)
1000	27.8	89.2
950	24.3	96.4
925	22.7	98.1
900	21.2	99.5
850	18.2	99.7
700	9.9	99.7
600	3.9	97.6
500	-3.5	95.3
400	-14.5	88.3
300	-28.2	85.5
250	-39.5	81.5
150	-69.2	75.5
100	-80.4	5.0
70	-77.9	5.0
50	-68.1	5.0
30	-55.7	5.0
10	-51.7	5.0

Table 4. Temperature and humidity profile used in this simulation.

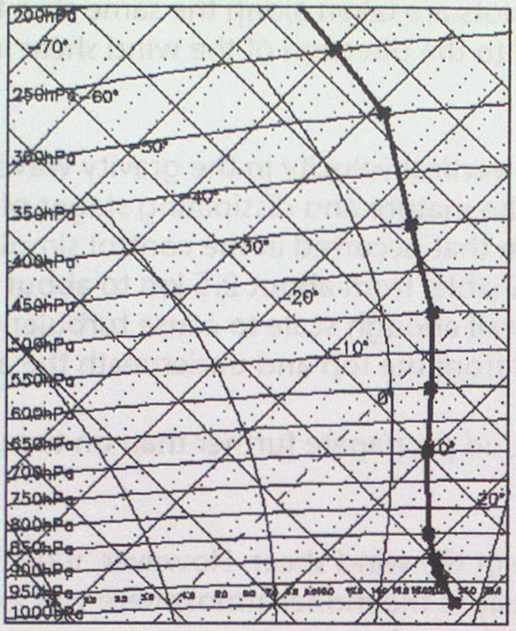

Figure 15. The temperature profile used in this simulation (plotted on a tephigram).

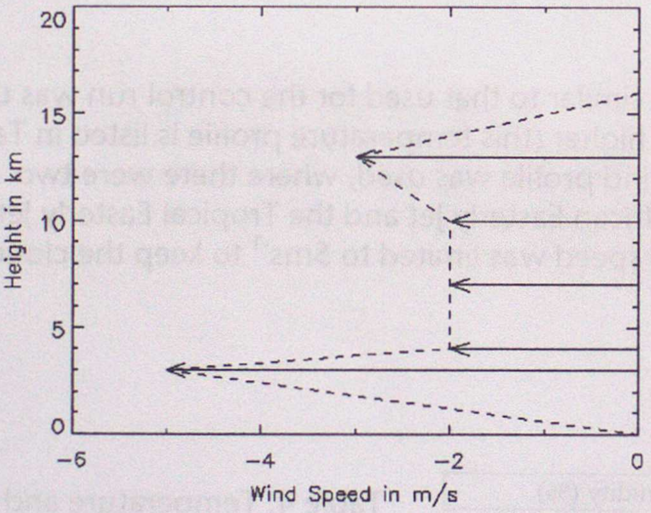

Figure 16. Wind profile used in this simulation.

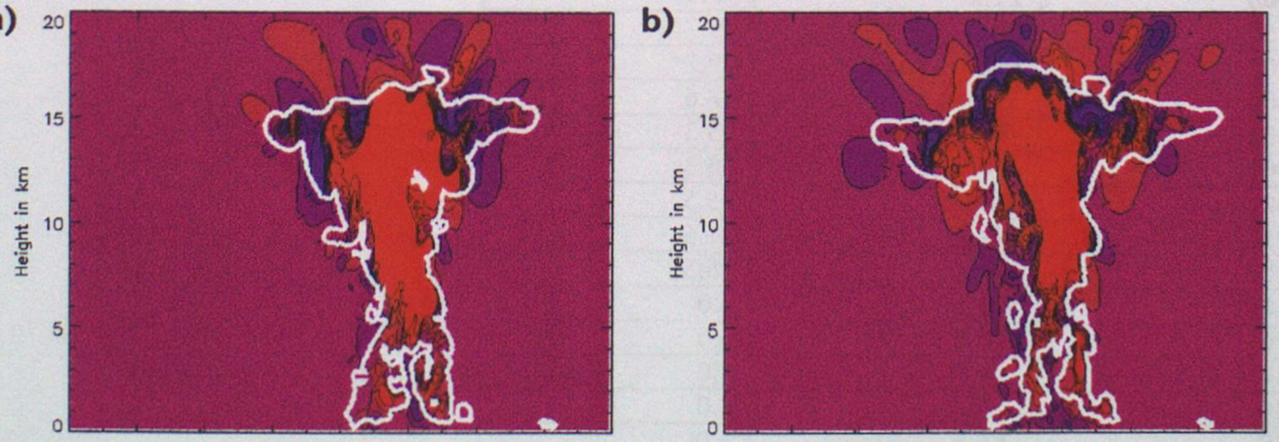

Figure 17. The vertical wind velocity (w) in ms^{-1} (a) 36 minutes and (b) 41 minutes after initiation. The contour intervals, colouring and outline of the cloud are as in Figure 7.

The vertical wind component through the centre of the grid at 36 minutes and 41 minutes after initiation is shown in Figure 17(a) and (b). In this simulation, the maximum magnitude of the vertical velocity in the gravity waves was about 8 ms^{-1}. This occurred just above the cloud top. These gravity waves had a wavelength of about 7 km, so the turbulence generated by these gravity waves probably would not affect aircraft. The maximum vertical velocity in the gravity waves above the anvil is about 3 ms^{-1}. These gravity waves have a wavelength of about 3 km, so the associated turbulence would affect aircraft.

The gravity waves on the downwind (left) side of the cloud have propagated further than on the upwind side of the cloud 41 minutes after initiation.

5 Conclusion and Recommendations for Further Work

Unfortunately, only very limited simulations could be performed due to restraints on number of grid points and the length of time needed for the Large Eddy Model to run. However, some preliminary conclusions can be drawn:

1) Gravity waves from the anvil and cloud top may cause turbulence that would affect aircraft. The largest vertical wind values in gravity waves occur in those over the cloud top and is of the order of 7ms^{-1}, however, these gravity waves also have longer wavelengths. These are more prevalent when there is wind shear.
2) The gravity waves close to the cloud beneath the anvil could also cause turbulence that could affect aircraft. These gravity waves appear to propagate further on the downwind side of the storm.
3) Apart from above the cloud, there is little or no turbulence surrounding the cloud system.

These results were produced from a very restricted set of simulations, which used idealised initial conditions. In addition, the grid resolution tests showed that the results are dependent on grid resolution, particularly rate of cloud growth and wavelength of gravity waves. For these reasons, these results must be viewed as preliminary results, which gives a rough idea of the pattern of turbulence around a cloud that may affect aircraft. Many more simulations should be performed before any firm conclusions can be made. For example:

1) the effect of changing the properties of the initialising cold pool should be investigated
2) the effect of a larger wind shear should be investigated
3) simulations should be made with observed profiles of wind and temperature taken from the midlatitudes and the tropics, and the results verified with turbulence measurements
4) gravity wave breaking above the cloud should be investigated, as this would cause considerable turbulence for aircraft
5) the turbulence field at a greater distance from the cloud should be investigated. One way to do this study with the current limitations of the Large Eddy Model and supercomputers, would be to run the model in 2D mode. The dissipation of the gravity waves may be a problem when running the model in 2D mode, so tests should be performed first to see if the results from running the model in 2D mode are meaningful.

References

L. B. Cornman, C. S. Morse, and G. Cunning, Real-Time Estimation of Atmospheric Severity from In-Situ Aircraft Measurements. Journal of Aircraft, Vol. 32, No. 1, pp171-177 (1993)

S.H. Derbyshire, A.R. Brown, A.P. Lock, 1994. TDN 213: The Met Office Large Eddy Simulation Model

Acknowledgements

The author wishes to thank the following for their help in this study:

Olaf Stiller of APR for setting up the LEM model for the study and for guidance, general discussions and suggestions during the study, and also for reviewing this paper;
Bob Lunnon, Steve Derbyshire and Glenn Shutts for general discussions and suggestions during the study;
Adrian Pickersgill for scanning in Figures 2, 3 and 4;
Clint Blight for help with the cross-section figures;
those on the Aviation Steering Group Committee for discussion and suggestions on the results of this project;
and Howard Lyne for providing some of the pictures of thunderstorms from the Met Office 'Met for Grads' training course.